Soils and Foundations 2015;55(1):143–153

HOSTED BY

ELSEVIER

The Japanese Geotechnical Society

Soils and Foundations

www.sciencedirect.com
journal homepage: www.elsevier.com/locate/sandf

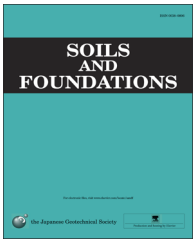

Pilot-scale modeling of colloidal silica delivery to liquefiable sands

Murat Hamderi[a,*], Patricia M. Gallagher[b]

[a]Royal Haskoning DHV-ELC, Istanbul, Turkey
[b]Dept. of Civil, Architectural and Environmental Engineering, Drexel University, Philadelphia, PA, USA

Received 2 June 2013; received in revised form 9 October 2014; accepted 21 October 2014
Available online 29 January 2015

Abstract

Passive site stabilization is a developing technology for the in situ mitigation of the risk of liquefaction without surface disruption. It involves the injection of stabilizing materials into liquefiable saturated sand. In this study, a pilot-scale facility (243 cm by 366 cm in plan × 122 cm deep) was used to inject a dilute colloidal silica stabilizer into liquefiable sand specimens. The grout advancement was monitored in real time using electrical conductivity cells embedded in the specimens. Injection rates ranging from 65 to 9000 ml/min/well were used to investigate the optimal rate of grout delivery. In tests with low injection rates, the delivery performance was low due to sinking, while at higher injection rates, sinking was less noticeable. After the treatment, the degree of grout penetration was evaluated by excavating the model. The in situ unconfined compressive strength was measured using a pocket penetrometer, and soil blocks were excavated for additional unconfined compressive testing. Moreover, the 3-D flood simulator, UTCHEM, was utilized to simulate the experimental results and to predict the injection rates for adequate stabilizer delivery. The results of the strength testing demonstrated that as little as 1% by weight of the colloidal silica provides a significant improvement in strength after a month of curing. The study also revealed the feasibility of delivering colloidal silica to liquefiable sands by implementing a large-scale treatment.

Keywords: Chemical grouting; Soil liquefaction; UTCHEM; Colloidal silica; Chemical transport; Groundwater

1. Introduction

Passive site stabilization is a technique for the non-disruptive mitigation of the risk of liquefaction at developed sites susceptible to liquefaction. The stabilization is performed by slowly by injecting a stabilizing material at the up gradient edge of a site and delivering the stabilizer to the liquefiable area using the groundwater flow augmented by injection and extraction wells (Fig. 1). The stabilizer used for this technique is colloidal silica (CS), which is an aqueous dispersion of microscopic silica particles that can be made to gel by adjusting the pH or ionic strength of the dispersion. Laboratory, bench scale, centrifuge and field tests have all demonstrated the effectiveness of the CS treatment against liquefaction and liquefaction-induced damage (e.g., Gallagher and Mitchell, 2002; Gallagher et al., 2007; Conlee et al., 2012). One feasibility issue remaining is the ability to deliver the CS uniformly over long distances. Gallagher and Lin (2009) demonstrated the ability to transport CS in adequate concentrations in 1-m, 3-m and 10-m-long one-dimensional column tests. Gallagher et al. (2007) successfully delivered CS to a 2-m-thick liquefiable zone over a 9-m-diameter test area.

The most difficult feasibility issue to address for passive site stabilization is whether the grout can be delivered uniformly to the liquefiable formation. In this research, we developed a pilot-scale box model to investigate the ability to deliver dilute

*Corresponding author.
E-mail addresses: mhamderi@yahoo.com (M. Hamderi), pmg24@drexel.edu (P.M. Gallagher).
Peer review under responsibility of The Japanese Geotechnical Society.

http://dx.doi.org/10.1016/j.sandf.2014.12.011

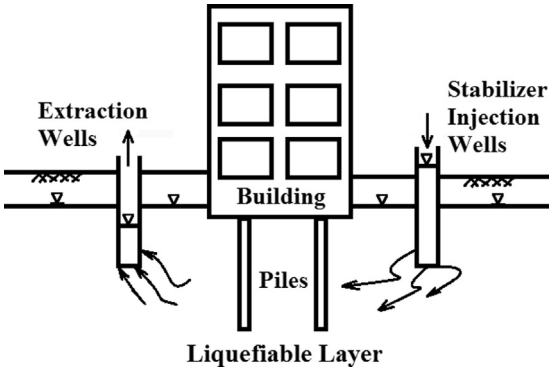

Fig. 1. Passive site stabilization concept.

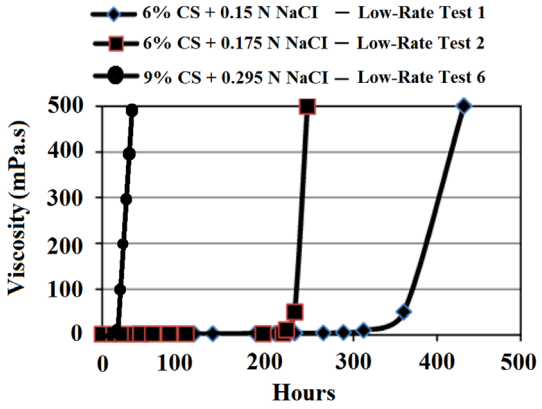

Fig. 2. Gel time curves of CS solutions used in this research.

CS in a large-scale laboratory model. This paper reports the results of pilot-scale injections in a 10-m^3 pilot-scale facility. In addition, we used UTCHEM, a finite difference numerical simulator that can account for various densities and viscosities, to model the results of experiments and to predict the optimal injection rates for adequate stabilizer delivery.

2. Colloidal silica properties and use in liquefaction mitigation

Colloidal silica (CS) is an aqueous dispersion of fine-sized, amorphous, nonporous and typically spherical silica particles in the liquid phase ranging from 5 to 100 nm in diameter (DuPont, 1997). During their manufacturing, CS solutions are stabilized with alkali solutions against gelation. Alkaline solutions make the nano particles ionize and repel each other. Gelation can be initiated by weakening the repulsive forces. This can be achieved by adjusting the pH level or the salt concentration. In most cases, adjusting the pH is cumbersome; therefore, the gelling time can usually be adjusted by only adding salt. In this study, Ludox-SM was selected from among the several types of CS available. Ludox-SM CS is a highly stable dispersion of 7-nm size SiO_2 particles. The dispersion has 30% SiO_2 by weight and a viscosity of about 5.5 mPa s at 20 °C. When CS is diluted to 6% with water, the density of the CS is about 1.035 g/cm^3 at 23 °C (density of tap water = 0.995 g/cm^3 at 23 °C) and the initial viscosity is between 1.05 and 1.6 mPa s (viscosity of tap water = 0.92 mPa s at 23 °C). The time to gelation can range from a few minutes to a few months (Gallagher and Mitchell, 2002). The general shape of the gel time curve is the same regardless of the gel time, as shown in Fig. 2, which presents the gel time curves for the experiments described later in this paper. The viscosity of the diluted CS remains low until just before gelation begins; this allows the grout to be injected for most of the induction period.

3. Previous studies on CS

3.1. Performance of CS in liquefaction mitigation

In the past fifteen years, numerous researchers have reported on significant improvements in the deformation resistance of

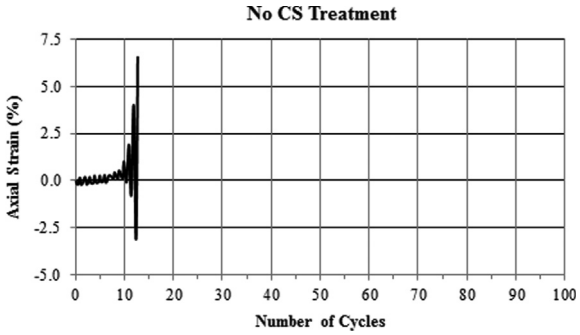

Fig. 3. Cyclic stress–strain behavior of untreated Monterey sand, relative density = 22%, CSR = 0.27 (Gallagher and Mitchell, 2002).

loose sands treated with CS in percentages from 2% by weight to 20% by weight (e.g., Kabashima and Towhata, 2000; Towhata and Kabashima, 2001; Gallagher and Mitchell, 2002). Loose sand treated with CS typically behaves similarly to dense sand and shows significant damping and cyclic mobility upon continued loading. Gallagher and Mitchell (2002) evaluated the performance of CS-treated and untreated samples by comparing their cyclic deformation resistance. The cylindrical Monterey sand samples were treated with 5% to 20% CS by weight. The samples were 7.5 cm in diameter by 15.9 cm in height. The Monterey sand had a d_{50} of 0.44 mm (d_{50} is the grain size corresponding to 50% passing). The void ratio of the samples was 0.70 which corresponded to a relative density value of 22%. The samples were compared in terms of strain development at a given CSR which is defined as the ratio of the maximum cyclic shear stress to the initial effective confining stress. A sinusoidal function with a period of 2 s was used for all tests. During the cyclic loading, untreated samples collapsed in 10–12 cycles (Fig. 3), whereas samples treated with 5% and 10% CS by weight could withstand at least 100 cycles, and they remained intact (Fig. 4a and b).

Conlee (2010) conducted a series of CS silica field injection tests to treat a 0.5-m-thick layer of poorly graded sand with silt against liquefaction. The injection was performed in a 9 m^2 area with an average injection rate of 5.7 l/min. Following the treatment, some dynamic shaking was introduced with dynamic shaker TRex. The induced accelerations ranged from 0.05 g to

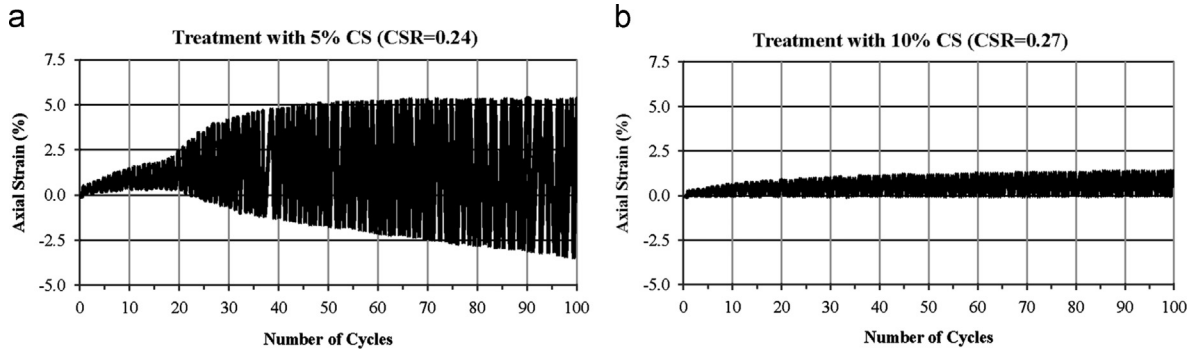

Fig. 4. Axial deformation during cyclic loading for treated sand: (a) 5% CS and (b) 10% CS (Gallagher and Mitchell, 2002).

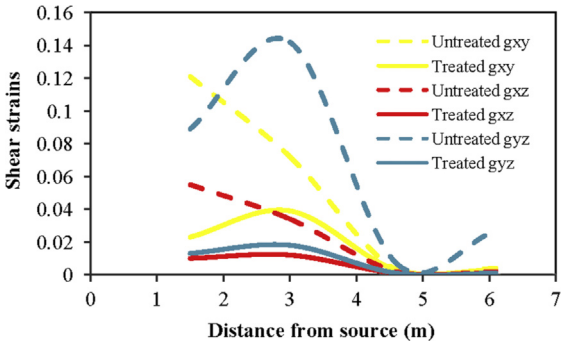

Fig. 5. Cross-plane shear strains (g_{xy}, g_{xz} and g_{yz}) calculated for CS-treated and untreated zones (by data from Conlee, 2010).

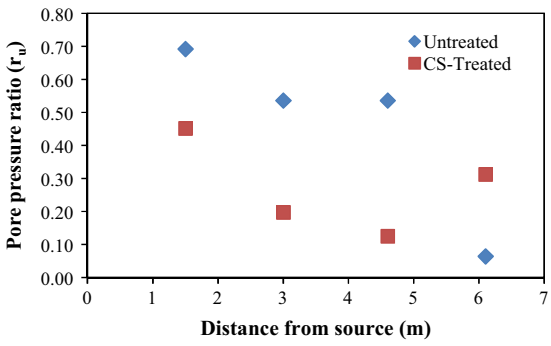

Fig. 6. Pore pressure ratios (r_u) of CS-treated and untreated zones (by data from Conlee, 2010).

0.4 g. A comparison was made between the treated and untreated test areas in terms of the measured shear strains and the pore pressure ratio, r_u. Cross-plane shear strains were calculated in horizontal (xy), vertical (xz) and (yz) planes (Fig. 5). The treated area demonstrated a clear reduction in shear strains compared to the untreated area. Similar to the shear strain values, pore pressure ratios (r_u) were considerably reduced in the treated area (Fig. 6). It was also reported by Conlee (2010) that if the CS injection is less than about 3700 ml/min/well, the CS had a tendency to sink downwards, due to its greater density compared to water.

Soil improvement by grouting is not restricted to CS. Other chemicals, such as acrylate liquid and calcium phosphate compounds, have recently been reported for the improvement of loose soils (Fattah et al., 2014; Kawasaki and Akiyama, 2013). Besides permeation grouting, compaction grouting is another option in which the injected liquid expands and compacts the surrounding soils rather than infiltrating through them. Wang et al. (2013) reported that when vibrations are applied along with compacting grouting, the improvement becomes about 4 times that of static compaction.

3.2. Delivery performance of CS

Early examples of CS injection include mainly permeability barriers. One of the early efforts for forming permeability barriers with CS was made by Moridis et al. (1996). It is reported that fairly uniform barriers from CS bulbs could be established using conventional grouting equipment.

Noll et al. (1992) formed a 0.9-m-wide permeability barrier with CS (Ludox-SM) in a 3.6 m × 1.8 m × 1.2 m sand container. The delivery was performed by three injection wells located in the middle of the sand container surrounded by three extraction wells on two opposite sides. After the injection, the box was opened and excavated to check the CS coverage.

Ludox CS was also used for the in-situ stabilization of a chemically contaminated area by Noll et al. (1993). The in-situ stabilization was accomplished by using an injection well in the center and six extraction wells aligned at a 6-m radius. During the test, the injection rate of the center well and the total extraction rate of the outer wells were set to 11.35 l/min. According to the prediction made with the MODFLOW program, the grout would travel towards the extraction wells. In contrast, Ground Penetration Radar (GPR) results indicated that the grout sank. This study provides one of the few examples demonstrating that CS grout is vulnerable to sinking.

Gallagher and Finsterle (2004) delivered Ludox-SM CS in a 0.31 m × 0.76 m × 0.27 m box with low head injection and extraction wells located on the upstream and downstream sides of the box, respectively. The model was later simulated by TOUGH2 (Pruess, 1991). The measured concentration and viscosity of the grout were compared with those calculated by TOUGH2. Generally, the predicted concentrations near the injection wells were similar to those observed during the actual test,

Fig. 7. Testing facility prior to low injection rate Test 2.

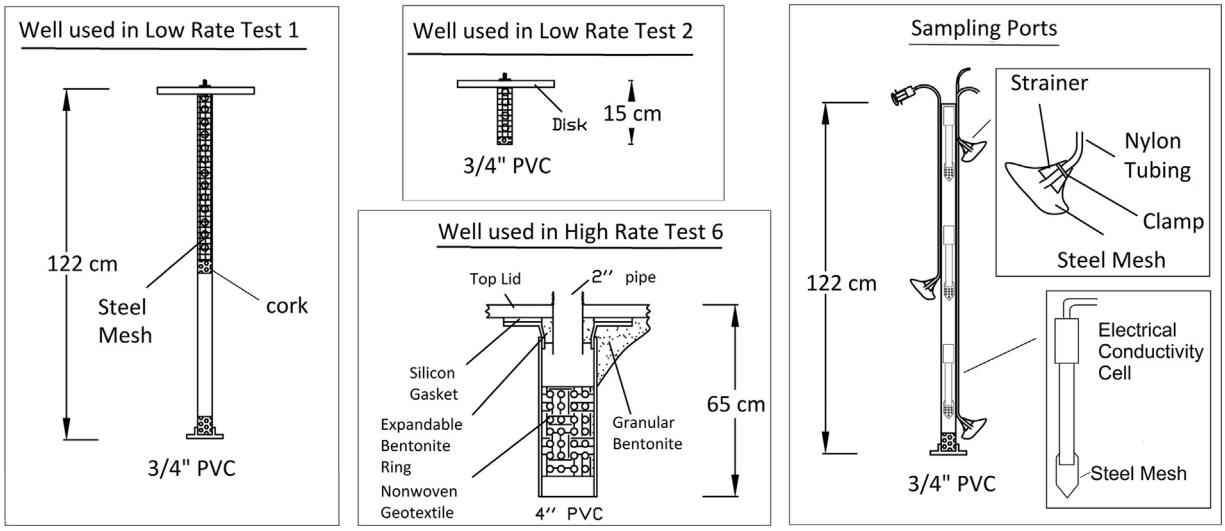

Fig. 8. Various types of wells and sampling ports.

whereas some deviations in concentration predictions occurred at remote locations. One of the shortcomings of this study is that the distance between the injection and the extraction wells was too small to observe any sinking potential. Hamderi and Gallagher (2013) investigated the sinking potential of CS using numerical methods, and they reported that the maximum feasible injection distance for CS lies in the range of 2.5 and 4 m.

4. Testing

The tests were grouped into two categories: low rate and high rate. The injection rates for the low rate and high rate tests were 65–130 ml/min/well and 2100–9600 ml/min/well, respectively. In addition to the laboratory tests, numerical simulations were performed using the flood simulator "UTCHEM".

4.1. Setup of low rate tests

Prior to placing the sand, the sampling ports and fifty electrical conductivity probes (Elmetron) were set in the pilot scale facility. For the low rate tests, 55 sampling ports were spaced at 50 cm and 30 cm intervals along the length and the width of the container, respectively. The sampling ports are labeled in Fig. 7 and details are shown in Fig. 8. A total of 60 hopper lifts were used to place 15 t of filter sand, which produced a loose sand layer with a relative density and hydraulic conductivity of 22% and 1.8×10^{-1} cm/s, respectively. The minimum and maximum void ratios for the filter sand were 0.48 and 0.81, respectively. The sand placement method was inspired by Vaid and Negussey (1998), who reported that when sand is freely poured onto water, it is

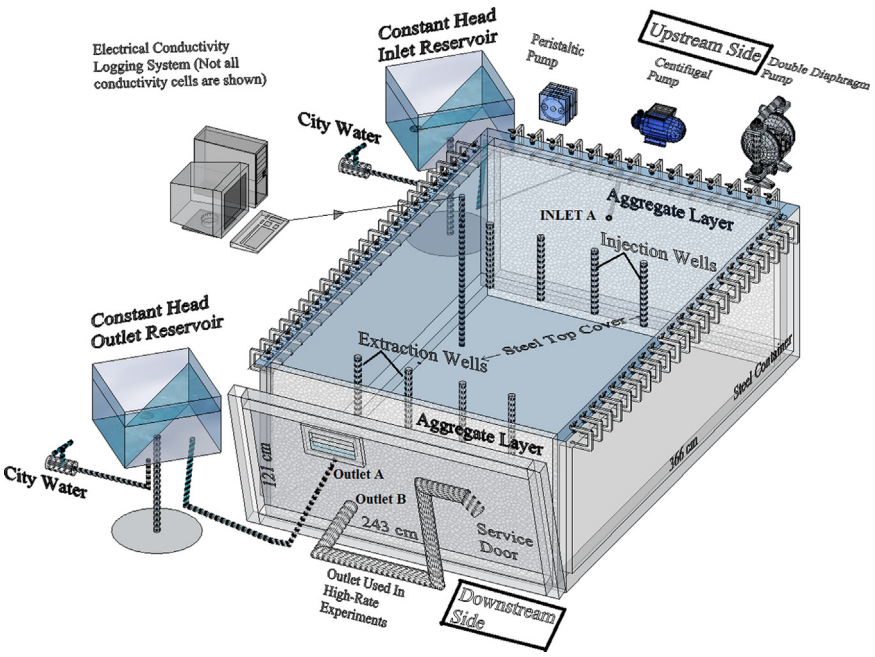

Fig. 9. General setup of the facility.

uniformly deposited regardless of the drop height. After the specimen preparation, an overall water flow through the specimen was established using constant head tanks. The overall flow through the specimen was established approximately 7 days prior to the first test in order to saturate the specimen as fully as possible and to simulate a baseline groundwater flow regime.

4.2. Execution of low rate tests

The main purpose of the low rate tests was to investigate the possibility of delivering CS at a total injection range of 260 ml/min. Grout was injected through 4 injection wells which were located about 130 cm away from the upstream side (Fig. 9). Additionally, 4 extraction wells were located on the downstream side to augment the grout flow. The details of these wells are given in Fig. 8. The continuity of the medium during the testing period was maintained by constant head reservoirs which fed the system continuously through Inlet A and Outlet A (Fig. 9). Aggregate layers were located at both extremes of the container in order distribute the flow over the entire section.

In total, two low rate tests were performed. In low rate test 1, grout was injected at a rate of 65 ml/min/well, whereas the same amount was extracted through the extraction wells from the downstream side. In total, a 0.4 pore volume of grout (about 1500 l) was prepared and planned for injection in 4 days. The gelation time for the test was about 12 days, which would allow extra time for the gelation in case some difficulties were encountered in the running test. The CS content of the solution was 6% by weight. The density of the CS solution was 1.04 g/cm^3.

Conlee (2010) reported that CS could easily be injected on site when the viscosity was below 4 mPa s. Accordingly, before each test, CS solutions containing various NaCl concentrations were prepared in order to determine the required NaCl concentration at which the viscosity during the injection phase would remain below 4 mPa s.

During low rate test 1, after 680 l of grout were injected, the sampling data indicated that the grout was sinking rather than moving horizontally. Consequently, the injection was stopped and the grout was flushed out of the sand for two days so that a second test could be performed on the same specimen.

The authors hypothesized that the sinking occurred due to the relatively higher density of the dilute CS compared to water, sand with high permeability (0.18 cm/s), the low injection rate, the low relative density, the long injection wells and leakage around the well annulus.

In order to address the hypothesized reasons, some modifications were made in low rate test 2, such as increasing the relative density from 22% to 48%, using shorter wells and doubling the injection rate.

During low rate test 2, about 1000 l of 6% CS (by weight)—0.175 N NaCl solution were injected in four and a half days. The concentration of CS, interpreted from the conductivity cell data tests, is plotted in Fig. 10. Despite the improvements, the CS sank in a similar manner to that which was observed in low rate test 1. After the excavation, it was also observed that silica was present in the bottom of the model, which agreed with the sampling and electrical conductivity cell results.

5. UTCHEM numerical tests

After sinking behavior was observed in the low injection rate experiments, numerical experiments were performed to

determine the optimal rates and pressures for injecting the CS that would result in a horizontal, rather than vertical, delivery. UTCHEM 9.2, which is a three-dimensional finite difference chemical flood simulator developed by the University of Texas at Austin, was used to model the CS injection (CPGE, 2000). In addition, the applicability of UTCHEM to 1-dimensional CS flow simulations was reported by Hamderi et al. (2014).

5.1. UTCHEM modeling parameters

Low rate test 2, with an injection rate of 130 ml/min/well, was used as a baseline model for the predictive UTCHEM runs. Numerical tests were run at the injection rates of 130, 378, 946, 1893, 3785, 5678 and 7570 ml/min/well. A constant pressure boundary (atmospheric pressure) was assigned to the downstream side, whereas the right boundary on the upstream side was impermeable.

CS was incorporated in UTCHEM by assigning viscosity, density and full solubility parameters to the oleic component present in UTCHEM. The assigned viscosity and density were 1.4 mPa s and 1.039 g/cm^3, respectively. During the low rate experiments, the viscosity was stable around 1.4 cP at 23 °C (0.92 mPa s for tap water) and increased by less than 5% during the injection. Therefore, a constant viscosity value was used for the numerical simulations. Additionally, a permeability value of 0.14 cm/s (128,800 mD in UTCHEM) and a porosity value of 0.39 were assigned to the aquifer (1 mD = 10^{-15} m^2).

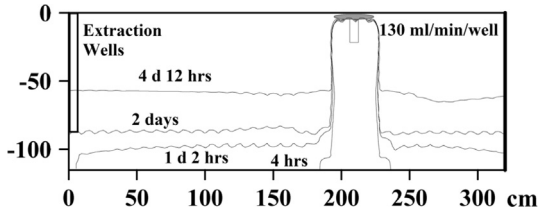

Fig. 10. Concentration distribution during low rate test 2 (Injection rate = 130 ml/min/well).

5.2. Results of UTCHEM numerical tests

Fig. 11 demonstrates the CS concentration contours in the numerical tests after 1/2 the pore volume was injected.

Based on the plots presented in Fig. 11a and b, CS grout tends to sink when the injection rate is between 130 and 946 ml/min/well. However, when the injection rate is higher (Fig. 11c and d), such as in the range of 1893 to 7570 ml/min/well, grout tends to advance horizontally. In other words, the grout advancement pattern shifts from "sinking" to "horizontally moving" at injection rates between 946 and 1893 ml/min/well. In addition, the concentration pattern predicted by UTCHEM at the injection rate of 130 ml/min/well is similar to the one observed in low rate test 2 (Figs. 10 and 11).

6. High rate tests

Six high rate tests were performed. Details are summarized in Table 1. In the high rate tests, concrete sand was used. The placement of the sand was performed in a similar way to that in the low rate tests. The minimum and maximum void ratio for the concrete sand was 0.41 and 0.78, respectively. In the high rate tests, five of the tests used a NaCl tracer solution and one used 9% dilute CS by weight. During the high rate tests, the injection rates were increased to levels of 1700 to 9600 ml/min/well. Based on the numerical modeling results, the required injection pressures were anticipated to be about 50 kPa. Given that the depth of the model was only

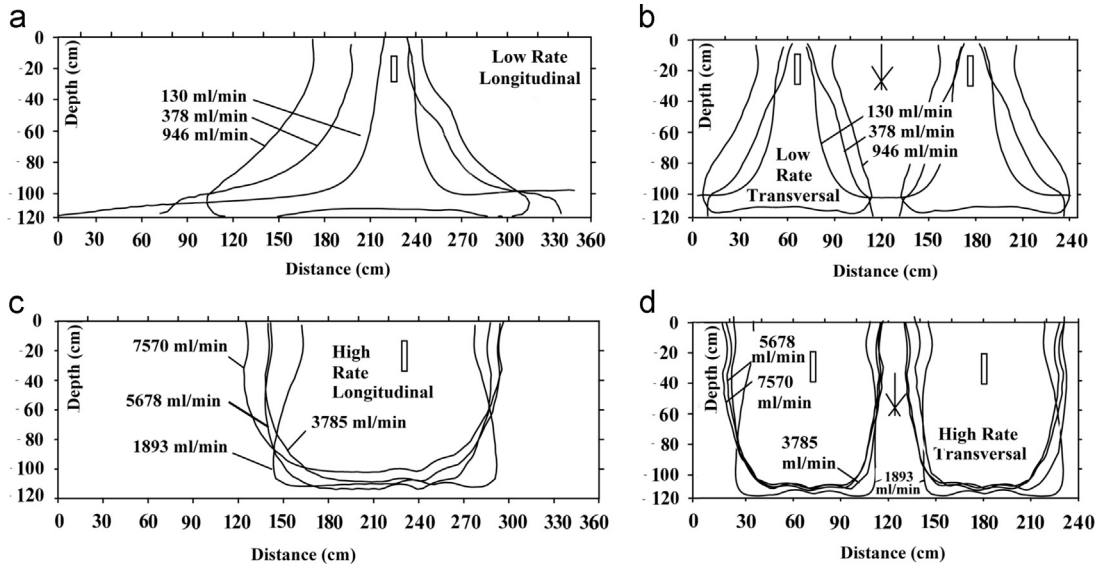

Fig. 11. Advancement of grout plume at different injection rates in a UTCHEM simulation—(a) and (b) on a longitudinal plane passing through one of the two injection wells, (c) and (d) on a transversal plane passing through both injection wells; each line shows the front end of CS grout for various injection rates in ml/min/well immediately after half the pore volume of grout was injected.

Table 1
Injection rates for high rate tests

	Test 1	Test 2	Test 3	Test 4	Test 5	Test 6
Avg. Inj. Rate (ml/min/well)	5800	4400	5600	2100	9600	6800
Volume Injected (l)	1752	3842	4133	4133	4088	4182
Volume Injected (pore volume)	0.4	1.0	1.1	1.1	1.0	1.1
Injection Duration (min)	150	442	366	975	213	308
Max. Inject. Press. per Well (kPa)	1.3	1.2	13.1	7.9	22.1	49.6
Grout Type/Density (g/cc)	salt/1.02	salt/1.063	salt/1.063	salt/1.063	salt/1.063	CS/1.063
Concentration (g/l)	26.5	82	82	82	82	9 wt% CS + 0.295N NaCl
Pump Type	1/2 Hp Centrifugal	1/2 Hp Centrifugal	Air Double Diaphragm	Air Double Diaphragm	Air Double Diaphragm	Air Double Diaphragm

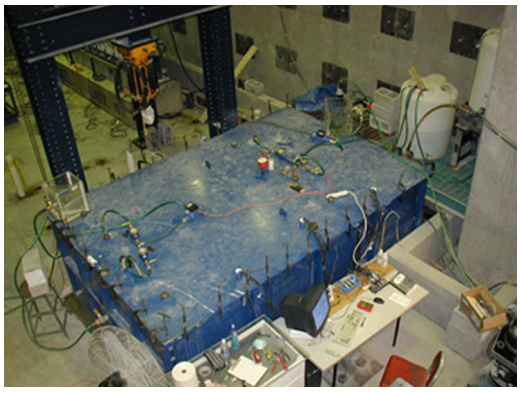

Fig. 12. Testing facility prior to high rate test 1.

about 1.2 m, it was necessary to fabricate a pressure cover so that higher injection pressures could be used. The steel cover, constructed of a 1.25-cm steel plate, was affixed to the specimen box using side clamps (Figs. 9 and 12). To prevent leakage through the cover, a 7-cm-thick C/S bentonite layer was placed on top of the sand layer. C/S bentonite is a granular bentonite product composed of polymer-free dried bentonite clay in various mesh sizes. In our tests, it swelled when it was exposed to water, creating a seal that was generally effective at preventing leakage.

Some grout return was detected around the annulus of the injection wells despite sealing around them with bentonite.

During the tests, injection pressures and tail water NaCl concentrations were measured. Due to the presence of the cover, the manual sampling ports could not be used; however, the electrical conductivity probes that were affixed to the sampling ports were used to monitor the electrical conductivity. Due to the corrosive nature of the NaCl tracer, many of the electrical conductivity cells stopped functioning as the tests progressed. While measurements in the remaining cells continued to be recorded, the best conductivity results were obtained in high rate test 1. By the time high rate test 6 was started, only three of the electrical conductivity cells were operational.

After the CS injection was completed (high rate test 6), the specimen was allowed to cure for 25 days prior to excavation. The model was excavated in vertical slices. A vertical surface was excavated every 0.3 m. At each vertical sampling surface, approximately 200 pocket penetrometer readings were taken in a grid pattern using a Geotest® soil penetrometer. A pocket penetrometer is a spring-operated device used to measure compressive strength in kg/cm^2. Since the electrical conductivity cells malfunctioned, the penetrometer readings were subsequently used to estimate the final concentration distribution in this experiment. In addition, at each vertical sampling surface, four soil blocks (0.30 m × 0.30 m × 0.15 m) were excavated and sealed in plastic wrap and aluminum foil for subsequent testing. Unconfined compression testing was done on 24 cylindrical specimens cut from the block samples. Red food coloring also assisted in assessing the coverage achieved by the CS.

6.1. Results of high rate test 1

As each high rate test was completed, it was simulated using UTCHEM to compare the results. Major aspects of the tests, such as the simulation of outlets and the aggregate layer on the downstream side, the injection and extraction wells and the leakage, were included in the model to improve the simulation accuracy.

A constant pressure boundary with permeable properties was assigned to the downstream side (Fig. 13), whereas the right boundary on the upstream side was set to be impermeable.

In UTCHEM, an intrinsic permeability value of 31,280 mD (1 mD = 10^{-15} m^2), which corresponds to a hydraulic conductivity value of 0.0034 cm/s, was assigned to the sand layer. The 5-cm-diameter outlet in the actual test was simulated with a 5 cm × 20 cm × 20 cm cell which had a comparatively high intrinsic permeability of 2500,000 mD.

Before the experiment, it was expected that the tracer solution would travel from the injection well to the extraction well and the outlet. These routes are marked as “2” and “1” in Fig. 13. About 20 min into the experiment, the bentonite seal around the extraction wells failed, resulting in the clogging of the wells. The broken seal around the top of the well provided an additional pathway for the tracer travel, which is marked “3” in Fig. 13a. This phenomenon was modeled in UTCHEM by replacing the extraction wells with point wells at the

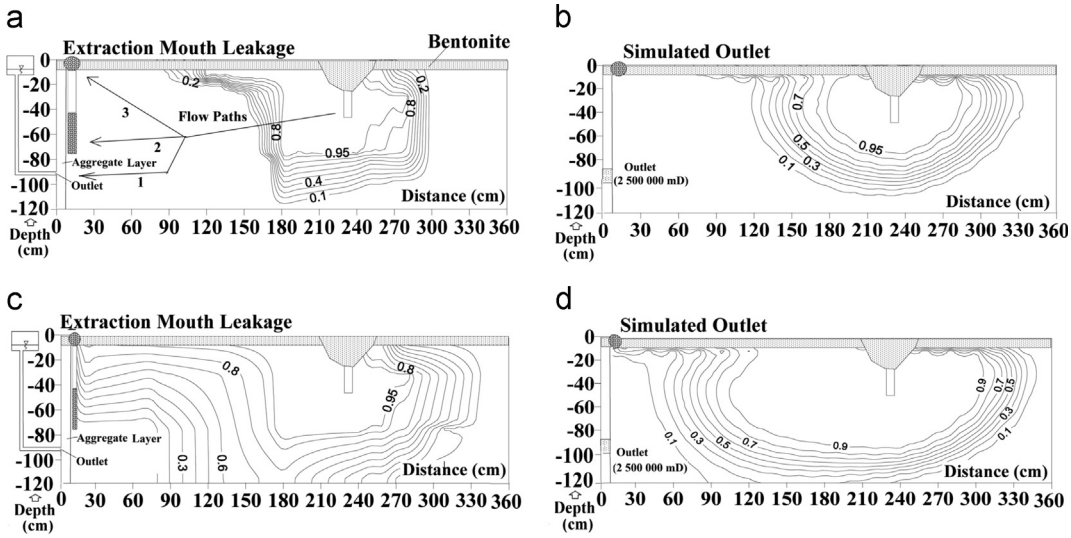

Fig. 13. Distribution of grout concentration in high rate test 1—(a) measured @ $t=80$ min, (b) simulated @ $t=80$ min, (c) measured @ $t=150$ min and (d) simulated @ $t=150$ min.

surface, which are labeled in Fig. 13b and d as "simulated outlet". Nevertheless, the measured and simulated distributions of NaCl at $t=80$ min and $t=150$ min were in fairly good agreement (Fig. 13). The remainder of the NaCl tracer tests showed similar results and are not reported here.

6.2. High rate test 6 (with colloidal silica)

In the final high injection rate experiment, most of the electrical conductivity cells had already stopped working, so the delivery performance of CS had to be evaluated in terms of the final CS distribution. The final concentrations were inferred in the following ways: (1) from pocket penetrometer readings taken as previously described; (2) from electrical conductivity measurements at the three functional electrical conductivity cells in the specimen and at the tail water outlet; and, (3) by correlating the penetrometer readings and unconfined compression test results performed on CS grouted sand samples.

The results of the laboratory pocket penetrometer tests resulted in a linear relationship between the penetrometer dial readings and the percentage of CS (Fig. 14).

This relationship was used to estimate the CS concentration at the penetrometer sampling points in the treated specimen using the following formula:

$$CS\% = \frac{P_{\text{point}}}{P_{\text{well}}} \times 9\ \% \tag{1}$$

where P_{point} = pocket penetrometer reading at a point, P_{well} = pocket penetrometer reading around the well and "9%" is the batch or well concentration of CS. Then, the final CS distribution in the specimen was calculated by inserting the measured values into Eq. (1).

6.3. Interpretation of CS concentration plot

Fig. 15a demonstrates the CS concentration plots on a longitudinal plane that were calculated using the values

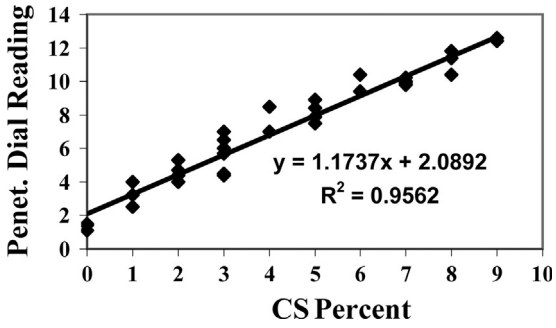

Fig. 14. Penetrometer dial reading and CS% relation.

obtained from the penetrometer method. Additionally, CS percentages predicted by the electrical conductivity method were marked on the same plot. The results of the two methods are in a good agreement.

During the delivery, it is hypothesized that CS grout traveled in a dispersed form along three different routes, as shown in Fig. 15a. In the vicinity of the wells, the measured CS concentrations are in the order of 9% by weight. Downstream from the wells, travel is through the sand layer (Route 1) or by leakage through the steel cover-bentonite interface (Route 2). The combination of these two travel paths resulted in a significant variation in concentration throughout the downstream section of the model. There is also some travel up gradient of the wells (Route 3) as a result of the injection pressures, even though there is no outlet on the up gradient edge of the model. Upstream from the injection well, the concentration decreases to about 1–2 % by weight CS, as expected.

The extent of the grout penetration along Route 1 is shown in Fig. 16a with red color. The leaky route is also shown in Fig. 16b. The existence of CS gel on the top of the bentonite layer indicates that the leakage occurred between the silicon well gasket and the steel cover. It is hypothesized that the contact between the cover and the silicon gasket was lost due

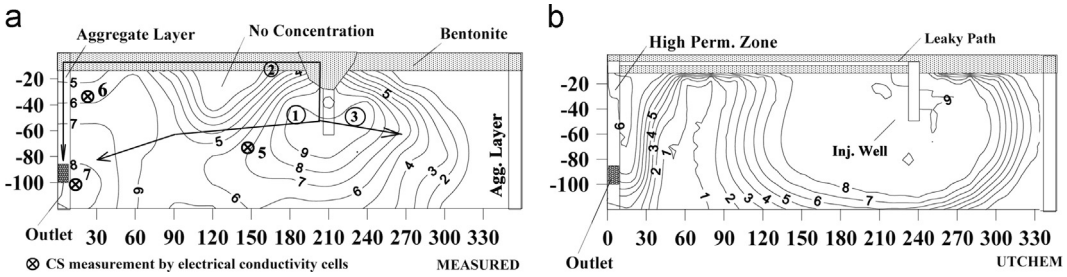

Fig. 15. Distribution of colloidal silica concentration in high rate test 6—(a) calculated from Eq. (1) and (b) simulated with UTCHEM.

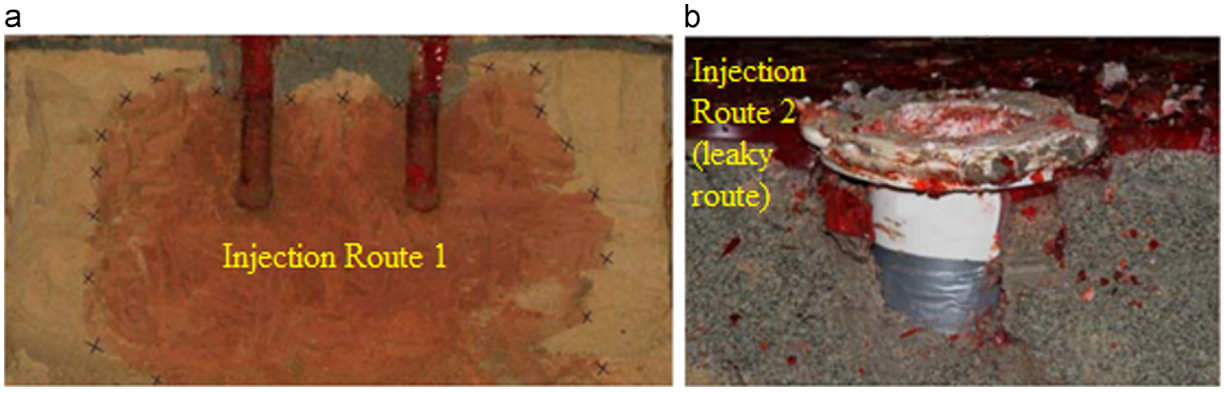

Fig. 16. (a) Grout penetration around injection wells and (b) leaked gel between the cover and the bentonite layer.

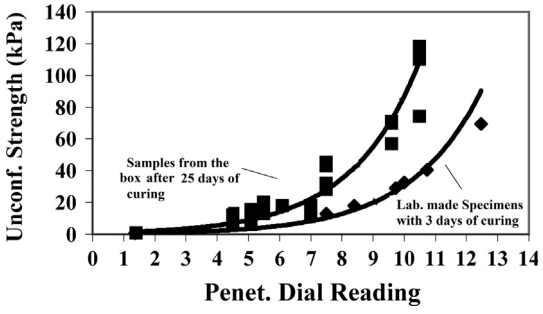

Fig. 17. Unconfined compression strength and penetrometer dial reading.

to the uplift force acting on the steel cover as a result of the bentonite swelling as it hydrated.

The results of the unconfined compressive tests from both the laboratory and the excavated model specimens are presented in Fig. 17. The laboratory specimens were cured for three days and plotted to the right of the excavated model specimens, which were cured for 25 days. The unconfined strength of the sand specimens treated with different CS concentrations fell in the range of 10 and 120 kPa. Based on Gallagher and Mitchell (2002), this level of improvement would be expected to be able to adequately mitigate the liquefaction risk for loose sands susceptible to earthquake loading.

6.4. UTCHEM simulation of the CS injection

In order to correctly model the experiment in UTCHEM, the amount of grout that leaked had to be estimated. There was no way to directly measure the percentage of grout that leaked through the steel–bentonite interface (Fig. 15a). As an alternative method, therefore, the percentage of leaked grout was estimated using the tail-water concentration measured in the outlet. In principle, the amount of grout travelling to the outlet is the sum of the amounts from Route 1 and Route 2. In UTCHEM, a parametric study was performed, in which different percentages of the injected fluid were sent along the different routes. This was achieved by setting up two injection wells and supplying each one with part of the total flow through the model. Route 2 was modeled by assigning high-permeability properties to the interface layer (10,000,000 mD) (Fig. 15b). Applying the law of conservation of mass, the total CS % was taken to be

$$\text{Total CS\%} = \text{leaked CS\%} + \text{injected CS\%} \quad (2)$$

By applying different combinations of flow to Routes 1 and 2 in each UTCHEM run, different tail water concentrations were obtained. They are shown in Fig. 18 along with the observed tail-water CS concentration. The closest match between the measured and the simulated data was achieved at "70% leaked—30% injected case". The final CS concentration in the "70% leaked—30% injected" case is also plotted in Fig. 15b and shows a fairly good match with the calculated concentrations.

6.5. Viscosity and injection pressure prediction by UTCHEM

The viscosity of the CS in the mixing tank was measured during the 277 min of injection (Fig. 19). We used this curve

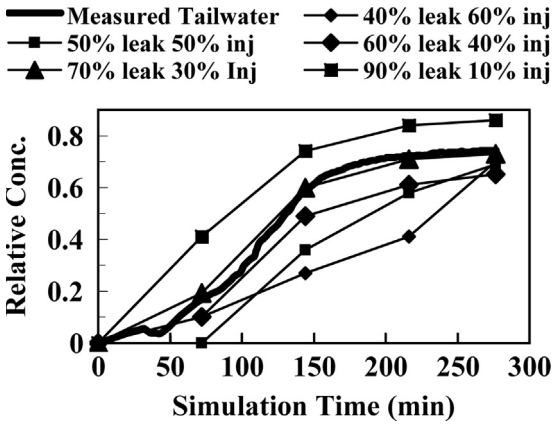

Fig. 18. Tailwater concentrations for different combinations of leak and injection rates in high rate test 6.

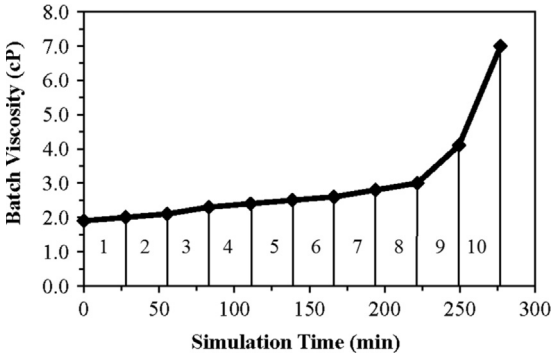

Fig. 19. Viscosity of colloidal silica in the mixing tank.

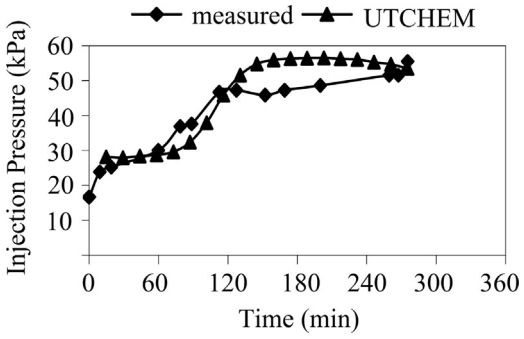

Fig. 20. Measured and simulated injection pressures (kPa).

in UTCHEM to predict the injection pressures during the injection. The area below the curve was divided into 10 equal time periods of 27.7 min. During the injection, the viscosity varied between 1.9 mPa s and 7 mPa s. For the UTCHEM analysis, an average viscosity value of 2.85 mPa s in 10 equal time periods was used. In UTCHEM, assuming that water and CS are fully miscible in the liquid phase, the viscosity at a point "μ_p" was estimated with the following formula:

$$\mu_p = \mu_w V_w + \mu_{cs} V_{cs} \quad (3)$$

where μ_w = viscosity of water at 23 °C = 0.92 mPa s, μ_w = average viscosity of the batch = 2.85 mPa s, V_w = volumetric ratio of water in the liquid phase, V_{cs} = volumetric ratio of CS in the liquid phase and $V_w + V_{cs} = 1$. This analysis resulted in a similar injection pressure trend between the simulated and the measured data (Fig. 20).

7. Conclusions

We developed a 10-m^3 pilot-scale box model to investigate the ability to inject dilute CS at a large-scale laboratory facility. In low concentrations, colloidal silica can adequately mitigate the liquefaction risk in loose sands by cementing individual grains together and immobilizing the pore fluid. In addition, it has a low initial viscosity and a wide range of controllable gel times, so that it can potentially be injected over longer distances than conventional grouts, resulting in the larger spacing of delivery wells.

One of the challenges associated with delivery over long distances is to prevent sinking of the colloidal silica prior to its reaching the desired location. Colloidal silica has a density slightly higher than water; consequently, it will always have a tendency to settle due to gravity. Therefore, it is necessary to select an injection method such that the horizontal travel component exceeds the vertical travel component. In addition, the gel time must be selected so that the viscosity remains low until the colloidal silica reaches the desired location and then increases in time to prevent gravitational settling. Our experiments show that low injection rates (<1900 ml/min/well) result in gravitational settling, but increasing the injection rates to between 1900 and 7600 ml/min/well result in sufficient horizontal pressures to adequately deliver an appropriate concentration of dilute CS to mitigate the risk of liquefaction. The viscosity only needs to increase to about 4 cP to prevent additional stabilizer movement once the target location is reached (Gallagher and Lin, 2009).

Based on our findings, the pocket penetrometer provided a good correlation for the percentage of CS in the treated sand. Although we did not do cyclic testing on the treated specimen, Gallagher and Lin (2009) established that the unconfined compression strength could be used as an index test to determine if adequate treatment has been achieved. In this research, we show that the pocket penetrometer can also serve as an index test. We also found that concentrations as low as 1% by weight CS provided sufficient cohesion to bind the sand after a relatively long curing time. Future research will investigate if the minimum concentration of 5% by weight suggested by Gallagher and Mitchell (2002) could be reduced.

The incorporation of viscosity and density effects in UTCHEM provides fairly successful numerical simulation results. The grout concentrations and the required injection pressures can be estimated at every calculation interval. The required injection pressure is important for predicting the limits of grout injection without exceeding the allowable grouting pressures in various sands.

Experimentally, we found that it was difficult to model the stabilizer delivery without having the ability to increase the confining pressure on the specimen. We modified the facility to include a cover that would permit higher levels injection pressure; it worked with moderate success, but leakage was

still experienced around the wells and through the granular bentonite layer.

The CS stabilizer is a viable option for the passive stabilization of soils that underlay existing structures and are difficult to treat by conventional ground improvement methods. The results of these pilot-scale experiments support the findings from prior research by demonstrating the ability to deliver dilute CS in adequate concentrations to improve the soil's resistance to seismic deformations.

In the high rate experiments, one pore volume of CS was not sufficient for establishing full concentrations in the treated volume. This was attributed to the high dispersion mechanism which was triggered by high injection rates.

Acknowledgements

Financial support for this research was provided by the National Science Foundation under Grant no. CMS-0238614. Any opinions, findings, conclusions and/or recommendations expressed in this material are those of the writer(s) and do not necessarily reflect the views of the project sponsors.

References

Center for Petroleum and Geosystems Engineering, 2000. Technical Documentation for UTCHEM-9.0: A Three-dimensional Chemical Flood Simulator. CPGE, University of Texas at Austin, Texas.

Conlee, C., 2010. Dynamic Properties of Colloidal Silica Soils Using Centrifuge Model Tests and a Full-Scale Field Test. Drexel Univ., Philadelphia, PA (Ph.D. Thesis).

Conlee, C., Gallagher, P.M., Boulanger, R.W., Kamai, R., 2012. Centrifuge modeling for liquefaction mitigation using colloidal silica stabilizer. J. Geotech. Geoenviron. Eng. 138 (11), 1334–1345.

DuPont, 1997. Ludox CS: Properties, Uses, Storage, Handling and Product Information. Delaware, Wilmington.

Fattah, M.Y., Al-Ani, M.M., Al-Lamy, M.T.A., 2014. Studying collapse potential of gypseous soil treated by grouting. Soils Found. 54-3, 396–404.

Gallagher, P.M., Mitchell, J.K., 2002. Influence of colloidal silica grout on liquefaction potential and cyclic undrained behavior of loose sand. Soil Dyn. Earthquake Eng 22, 1017–1026.

Gallagher, P.M., Finsterle, S., 2004. Physical and numerical model of CS injection for passive site stabilization. Vadose Zone J. 3, 917–925.

Gallagher, P.M., Conlee, C.T., Rollins, K.M., 2007. Full-scale field testing of colloidal silica grouting for mitigation of liquefaction risk. J. Geotech. Geoenviron. Eng. 133 (2), 186–196.

Gallagher, P.M., Lin, Y., 2009. Colloidal silica transport through liquefiable porous media. J. Geotech. Geoenviron. Eng. 135 (11), 1702–1712.

Hamderi, M., Gallagher, P.M., 2013. An optimization study on the delivery distance of colloidal silica. Sci. Res. Essays 8 (27), 1314–1323.

Hamderi, M., Gallagher, P.M., Lin, Y., 2014. Numerical model for colloidal silica injected column tests. Vadose Zone J.http://dxdoi.org/10.2136/vzj2013.07.0138.

Kabashima, Y., Towhata, I., 2000. Improvement of dynamic strength of sand by means of infiltration grouting. In: Proc. Third International Conference on Ground Improvement Techniques—2000. Singapore, pp. 203–208.

Kawasaki, S., Akiyama, M., 2013. Enhancement of unconfined compressive strength of sand test pieces cemented with calcium phosphate compound by addition of various powders. Soils Found. 53-6, 966–976.

Moridis, G.J., Apps, J., Persoff, P., 1996. A Field Test of a Waste Containment Technology Using a New Generation of Injectable Barrier Liquids. 18–23. Spectrum '96, Seattle, WA (August).

Noll, M.R., Bartlett, C., Dochat, T.M., 1992 In situ permeability reduction and chemical fixation using CS. In: Proceedings of the Sixth National Outdoor Action Conference on Aquifer Restoration. National Groundwater Association, Las Vegas, pp. 443–457.

Noll, M.R., Epps, D.E., Bartlett, C.L., Chen, P.J., (1993) Pilot field application of a CS gel technology for in situ hot spot stabilization and horizontal grouting. In: Proceedings of the Seventh National Outdoor Action Conference, National Ground Water Association, Las Vegas, pp. 207–219.

Pruess, K., 1991. TOUGH2—A General Numerical Simulator for Multiphase Fluid and Heat Flow. Lawrence Berkeley Laboratory, Berkeley, CA (Report LBL-29400).

Towhata, I., Kabashima Y., 2001. Mitigation of seismically-induced deformation of loose sandy foundation by uniform permeation grouting. In: Proc. Earthquake Geotechnical Engineering Satellite Conference, 15th International Conference on Soil Mechanics and Geotechnical Engineering, Istanbul, Turkey, pp. 313–318.

Vaid, Y.P., Negussey, D., 1998. Preparation of reconstituted sand specimens. In: Donaghe, R.T., Changey, R.C., Silver, M.L. (Eds.), Advanced Triaxial Testing of Soil and Rock, ASTM 977. American Society for Testing and Materials, Philadelphia, pp. 405–417.

Wang, S.Y., Chan, D.H., Lam, K.C., Au, S.K.A., 2013. A new laboratory apparatus for studying dynamic compaction grouting into granular soils. Soils Found. 53-3, 462–468.